Colloids and Surfaces A: Physicochem. Eng. Aspects 240 (2004) 187–198

COLLOIDS AND SURFACES A

www.elsevier.com/locate/colsurfa

Reversible shear gelation of polymer–clay dispersions

Danilo C. Pozzo, Lynn M. Walker*

Department of Chemical Engineering, Center for Complex Fluids Engineering, Carnegie Mellon University, Pittsburgh, PA 15213, USA

Received 22 December 2003; accepted 12 April 2004

Abstract

Reversible, shear-induced gelation of semi-dilute aqueous colloidal dispersions consisting of monodisperse discoid particles (Laponite) and weakly adsorbing polymer (polyethylene oxide) is studied through a combination of small angle neutron scattering and oscillatory shear. When shaken the samples undergo a dramatic transition from a low viscosity fluid to a self-supporting, turbid gel. This complex non-linear behavior is found to occur over a narrow composition regime near a composition commensurate with saturation of the clay surface with polymer. Through a combination of SANS and rheology, shear gelation is found to occur through the deformation of large stable flocs that expose fresh surface area for the formation of new polymer bridges. At rest, the temporary shear-induced flocs slowly fractionate with time as the polymer desorbs from the clay surface. The shear-induced gelation is time reversible and strongly temperature-dependent suggesting that relaxation is an activated process. Samples showing shear induced gelation are also able to form stiff stable gels which are characteristically similar to pure clay dispersions.

Keywords: Gel; Nanoparticles; Polymer; Neutron scattering; Rheology

1. Introduction

An extensive number of studies are devoted to the topic of complex interactions between polymers and solid colloidal particles. Many of these works are driven by industrial interest resulting from the large number of products and processes involving multi-component mixtures. For example, the pharmaceutical, pulp and paper and petroleum industries routinely deal with polymer–particle dispersions. These complex mixtures are used as rheological modifiers, as additives in coatings, and to stabilize or flocculate colloidal systems. Additionally, the development of nanotechnology in fields such as biomedicine and materials science has resulted in renewed interest from academics and high technology companies. The behavior of dispersions at high and low polymer concentrations has been extensively studied and the stabilization and flocculation phenomena are now considered well understood [1]. Typically, the addition of an adsorbing polymer to a colloidal dispersion causes flocculation at low surface coverage and steric stabilization when the particle surface is saturated with polymer. However, the transition region between these two opposing scenarios represents a gray area where metastable states are often observed [2,3].

In the past, most studies have focused on systems in the limit where particles are much larger than the polymers and the polymer–particle interaction can be approximated as adsorption on a flat surface. Solid particles with well-controlled geometry in the size range of tens of nanometers or smaller are now accessible to the research community as standard materials. Studies on systems where the particles are comparable or smaller than the characteristic size of the polymers have great technological potential [4] but can result in unexpected adsorption behavior [5–7]. When the particle size is reduced, the adsorption behavior is affected by new phenomena related to increased curvature and surface area, enhanced particle mobility and topological constraints [8].

Discoid particles have flat surfaces and can show very different structures and particle mobility than spherical particles of similar size. Synthetic smectic clay particles (for example Laponite^{TM}, Saponite^{TM}) have been extensively studied in the last 5 years because of their complex phase behavior at very low concentration [6,7,9–16]. The behavior in the presence of water soluble polymers has also been studied for gels [13,14] and fluid dispersions [6,7,9,16]. Shear

* Corresponding author. Tel.: +1-412-268-3020; fax: +1-412-268-7139.
E-mail address: lwalker@andrew.cmu.edu (L.M. Walker).

0927-7757/$ – see front matter © 2004 Elsevier B.V. All rights reserved.
doi:10.1016/j.colsurfa.2004.04.040

transitions between these two states were recently reported for aqueous dispersions of Laponite and polyethylene oxide (PEO) at very low concentrations [2]. Over a narrow composition range, close to surface saturation, these samples exhibit abrupt thickening upon agitation. When shear stops, this dramatic increase in elasticity is followed by a very slow relaxation of the gels to the initial fluid state. Samples that exhibit this strong, but reversible, shear thickening have been dubbed "shake gels". The induced gels are very stiff and viscoelastic with properties that are qualitatively different from those of the pure clay dispersions. The properties of the samples before the shear gelation and after the complete relaxation are very similar to those of dilute colloidal dispersions with a viscosity similar to water. A similar shear effect is also observed with small silica particles in the presence of adsorbing polymer [3]. In both systems the shear gelation is reversible and it is observed near the surface saturation limit.

The mechanism for shear-induced gelation and the subsequent relaxation is interpreted as being caused by the formation of unstable polymer bridges that result in the creation of large elastic flocs. These physical bonds are naturally weak because they have been formed through the adsorption of a small number of polymer segments on new clay surface. This surface was made available to adsorption as a consequence of the shear deformation of stable aggregates. When the deforming stress is released, thermal motion of the components drives the slow desorption of these weakly bound segments and results in the fragmentation of the shear-induced aggregates. This is experimentally observed with a slow relaxation to the initial fluid state. The state reversibility is possible because only few polymer segments act as anchors that can easily desorb without the largely coordinated effort that is needed in multi-segment desorption. However, if a larger part of the chain adsorbs on the exposed surface, the polymer bridges become stable and flocs do not completely break up after relaxation. This would be observed as an irreversible flocculation and a dependence of sample properties on the sample history.

Even though the "shake-gel" dispersions are stable and do not flocculate with time, complete flocculation and separation of the solids from the solvent can be achieved by rubbing the samples between fingers. Therefore, the reversible gel state presents interesting possibilities in new separations technology. This state duality, sol and gel, may be useful in shear controlled flocculation of materials after they have been effortlessly transported and processed in sol form. This paper focuses on the characterization of the "shake-gel" effect through small angle neutron scattering (SANS) and rheology in order to improve in the microscopic gelation model that was previously presented [2].

Fig. 1a shows a pictorial representation of the shear induced gels and other phases that are observed as the PEO concentration is varied at a fixed clay concentration. At very low concentrations of PEO, most of the chains are adsorbed and bridging can only occur over a small fraction of the particle population. Because most of the particles are individual primary particles, the samples behave like pure clay dispersion of similar concentrations. This is the "stable sol" phase which is a stable, low viscosity solution. At higher

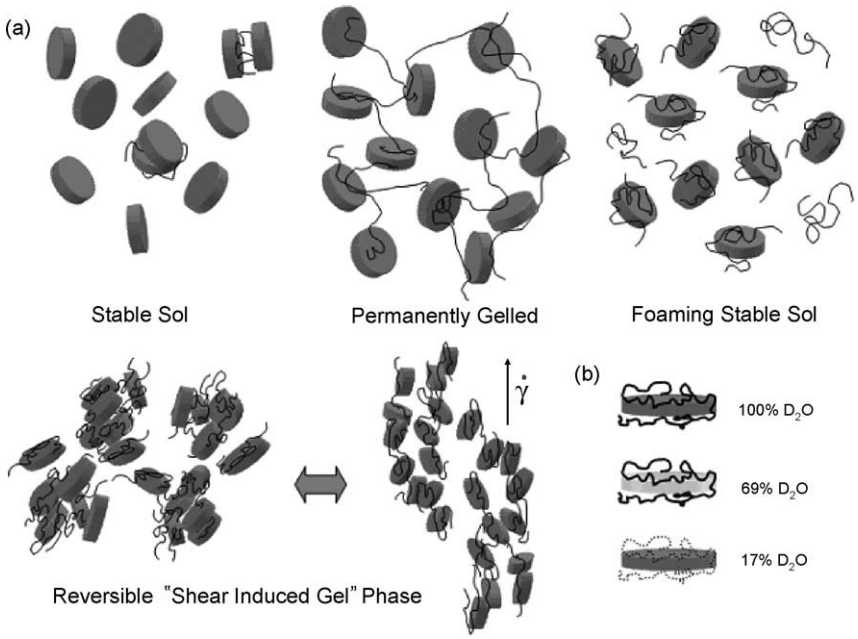

Fig. 1. (a) Pictorial sketch of various phases observed as the amount of polyethylene oxide is increased with respect to the total particle surface area. At low PEO concentrations, samples behave like pure clay dispersions. Increasing the polymer concentration creates permanently gelled samples with no shear-dependent structure. Near the saturation limit, shearing the samples creates stiff gels that can relax back to the initial fluid state. With excess PEO the samples are stable dispersions that foam upon agitation. (b) Sketch of contrast matching technique.

PEO concentrations but below the surface saturation, there is enough polymer to cause the macroscopic flocculation of the particles. These bridges are stable because the surfaces are not saturated with polymer. This is evidenced macroscopically as a turbid gel that shows no relaxation. This is the "permanently gelled" phase. As PEO concentrations are increased towards the concentration of surface saturation, the size of the aggregates decreases and the samples again become transparent sols. It is in this region that the shear induced gelation is observed. If PEO concentrations are further increased above the clay surface saturation values, the samples are transparent and fluid. A foam layer develops on agitation, which indicates the presence of free polymer chains in solution. These samples compose the "foaming stable sol" region.

In the absence of shear, colloidal particle movement is dominated by Brownian motion arising from collisions with solvent molecules. In the presence of a shear field the Peclet number is used to scale this random motion with respect to the hydrodynamic forces (Eq. (1))

$$Pe = \frac{\dot{\gamma}a^2}{D} = \frac{\dot{\gamma}a^3 6\pi\eta_0}{k_b T} \quad (1)$$

In this equation, a is the characteristic particle size, $\dot{\gamma}$ the characteristic shear rate, D the self-diffusion coefficient and η_0 the solvent viscosity. When this number is of order 1 or greater, the hydrodynamic forces become strong enough to compete with the thermal motion so that particle tumbling and stretching effects are observed. At $Pe \ll 1$ the particle motion is controlled by the thermal energy. Particles with size range in the tens of nanometers are not influenced by typical experimental shear rates (∼1000 l/s). Yet, because the Peclet number is a strong function of aggregate size, stable aggregates in the 100 nm size range are influenced by ordinary shear fields. Consequently, some degree of stable aggregation is required in shear-induced gelation and shear-induced flocculation of systems of nanoparticles.

This work aims to quantify this dramatic shear gelation effect and gain insight into the molecular gelation and relaxation mechanisms. Oscillatory strain rheology is used to characterize the time-dependent modulus after the gel state is induced. This procedure is used to evaluate the temperature and the sample age dependence of the gel relaxation. The linear and non-linear flow responses are analyzed through Lissajous phase plots during the measurement cycles of the gel relaxation. Characterization of the full frequency and strain spectrum becomes increasingly difficult because of the metastable nature of the gel state and because its relaxation occurs in the timescale of the experimental measurements. Small angle neutron scattering experiments are used to probe the aggregate microstructure in the gel state and after the relaxation.

SANS experiments have become standard tools in the determination of colloidal structure because of the short radiation wavelength and the neutron sensitivity towards light atoms. The scattering function for a three component interacting system is given by the scattering that arises from the individual components and the correlations between them as shown in Eq. (2)

$$I(q) = (\rho_1 - \rho_s)^2 S_{11}(q) + (\rho_2 - \rho_s)^2 S_{22}(q) + 2(\rho_1 - \rho_s)(\rho_2 - \rho_s) S_{12}(q) \quad (2)$$

Because of the additional scattering from correlations between the different components (S_{12}), the scattering from interacting systems is greater than the sum of the scattering of the pure components in solution. SANS also presents the possibility of variation of the scattering contrast through the choice of different molar amounts of isotopic solvents. When the molar average scattering length density of the solvent (ρ_s) is set to be equal to that of one of the dispersed components, the scattering arising from the molecular correlations of the third component is measured [5,6,14,16]. If the scattering at various contrast values is obtained from several experiments, it is possible to recover all the individual contributions to the total scattering. This powerful technique allows the determination of the structure of individual components in complex mixtures. A sketch of the contrast matching technique for this system is shown in Fig. 1b. In this work we make use of the opposite sign of the scattering length density of H_2O and D_2O. When the solvent is pure D_2O, the clay and the PEO are in contrast to the solvent and the scattering function contains information of both components. When the solvent is 69% D_2O and 31% H_2O the scattering length density of the solvent is equal to that of the clay particles and the collected scattering function is mostly dependent on the polymer structure. At 17% D_2O the scattering length density is matched to the polymer and the recovered function is mostly dependent on the particle structure. Contrast is experimentally verified by scattering of pure components in matched solvents. In the case of colloidal particles with adsorbing polymer, the correlated structure factors can also be used to obtain a segment concentration profile after assuming a functional form. Unfortunately, the scattering is heavily biased towards the regions of high segment concentration and is therefore inaccurate in determining the extension of polymer loops and tails.

2. Materials and methods

2.1. Sample preparation

Synthetic hectorite clay (Laponite XLG) was obtained as a gift from Southern Clay Products (Gonzalez, TX). This high purity grade has an empirical formula of $Na_{0.7}{}^{+}[(Si_8Mg_{5.5}Li_{0.3})O_{20}(OH)_4]^{-0.7}$. In dry form the particles are stacked together in form of tactoid columns which are readily hydrated. This eventually results in the complete exfoliation into individual monodisperse discs approximately 25–30 nm in diameter and 0.9 nm thick [6,7,10–12]. On dispersion in water, the hydrated sodium

ions are released from the surface of the particles forming an electrical double layer and resulting in a net negative surface charge. Laponite dispersions form clear gels at very low solids concentrations (∼3%, w/w) and fluid dispersions that show a slow time-dependent increase of the viscosity at lower weight fractions. The formation of these gels at such low weight fractions have been attributed both to the formation of "house of cards" fractal networks and to a glassy state due to kinetic caging of the particles from repulsive interactions [10–12]. Because of the slow evolution of the viscosity and the static Laponite gelation, the samples in this report were made at low Laponite concentrations and were freshly prepared no more than 30 min prior to each experiment. Preferential alignment in the samples could be expected due to the anisotropy of the primary particles and the imposed shear fields. Therefore, samples were checked for birefringence by placing between crossed polarizers before and after being sheared. The samples were not birefringent at rest, indicating that the concentrations used were below any isotropic to nematic phase transition boundary [15]. However, the samples that exhibited shear-induced gels showed static birefringence in the gel state that relaxed back to the initial non-birefringent state.

Poly(ethylene oxide) or PEO with a listed molecular weight of 300,000 g/mol was obtained from Aldrich Chemical Company (Milwaukee, WI) and was used as received. The polymer radius of gyration was determined to be 20.5 nm from SANS data and 21.7 nm from intrinsic viscosity measurements [17]. The samples were prepared by fully dispersing the clay in 18 MΩ Millipore filtered de-ionized water which is then mixed with a corresponding amount of a PEO stock solution. PEO stock solutions are prepared well in advance, ensuring complete dispersion of the polymer chains. It is of critical importance that the clay be added as the first component and allowed to fully disperse since the premature addition of polymer can prevent the full exfoliation of the tactoids and result in a considerable shift of the region of shear-induced gelation. The pH of the resulting samples was measured to be about 10, a pH at which the Laponite particles are stable and negatively charged [7]. SANS samples were prepared with 99.8% pure deuterated water obtained from Aldrich or in D_2O/H_2O mixtures so that the solvent was matched in scattering density (SLD) to either the PEO (17% D_2O, SLD $= 0.62 \times 10^{-6}\,A^{-2}$) or the Laponite (69% D_2O, SLD $= 4.2 \times 10^{-6}\,A^{-2}$). Scattering profiles from the pure components in and around contrast matching conditions were used to check the zero scattering solvent compositions.

2.2. Rheology

The rheological measurements are performed with an ARES (TA Instruments, New Castle, DE) strain-controlled rheometer using a Couette cell. In this configuration a cup of 34.0 mm in diameter acts as the rotor and a bob of 32.0 mm in diameter and 33.0 mm in length is the stator. Dynamic experiments are used to probe the mechanical properties of the system. In these experiments, the samples are subject to a small sinusoidal strain function ($\gamma = 1\%$) and the stress response is computed from a torque transducer connected to the stator. Large strain amplitudes ($\gamma = 10$–500%) are also used to identify the onset of the non-linear rheological response. The frequency of oscillation, $\omega = 1$ rad/s, is kept constant for all experiments. The temperature is controlled to within $\pm 0.1\,^{\circ}C$ by means of a fluid bath that circulates fluid around the bob. Sample evaporation is prevented by adding a thin coat of silicone oil. The rheological influence of the thin oil coating is found to be negligible.

2.3. Small angle neutron scattering

Measurements are performed at the NIST Center for Neutron Research in Gaithesburg, MD using the NG3 30 m SANS instrument. A quartz Couette cell with 1 mm gap is used for shear and relaxation measurements. The shear cell and its operation have been previously described in detail [18]. A neutron de Broglie wavelength of 6 A with a spread $\Delta\lambda/\lambda$ of 0.15 is used at various detector distances to gather full scattering profiles. Detector distances of 12.0, 4.0 and 2.0 m are used corresponding to Q-values between $0.004 < Q < 0.18\,A^{-1}$. All the data was appropriately reduced and set on an absolute scale with respect to open beam transmissions. Incoherent background intensity, measured at $Q > 0.1\,A^{-1}$ are subtracted from the corresponding profiles.

3. Results and discussion

3.1. Phase behavior

A phase diagram of the Laponite–PEO system has been presented previously [2] and is expanded and reproduced in our laboratory. Our phase diagram is shown in Fig. 2. The figure shows the observed phases as a function of clay concentration in weight percent and the mixture concentration given as Γ_t, the total mass of polymer per total area of clay surface. When plotted in terms of amount of polymer per particle surface area it is clear that the phase transitions from macroscopic flocculation to shear gelation and to stable sol are functions of the polymer surface coverage. If it is assumed that most polymer is adsorbed, the region of induced gelation is close to the expected surface saturation value for the PEO–Laponite system previously reported in the literature. Lal and Auvray used a core-shell model to obtain saturation adsorbed amounts for PEO of various M_w on Laponite RD [6]. More recently, Nelson and Cosgrove improved on the core-shell model by allowing the shell to extend on the sides of the clay particles [16]. This resulted in a more realistic model and better fit results. The authors found that the polymer adsorbs flatly and coats the clay particles with a larger shell on the sides (2.5–5 nm) than the shell normal to the surface (1.5 nm). Additionally, they found that the edge

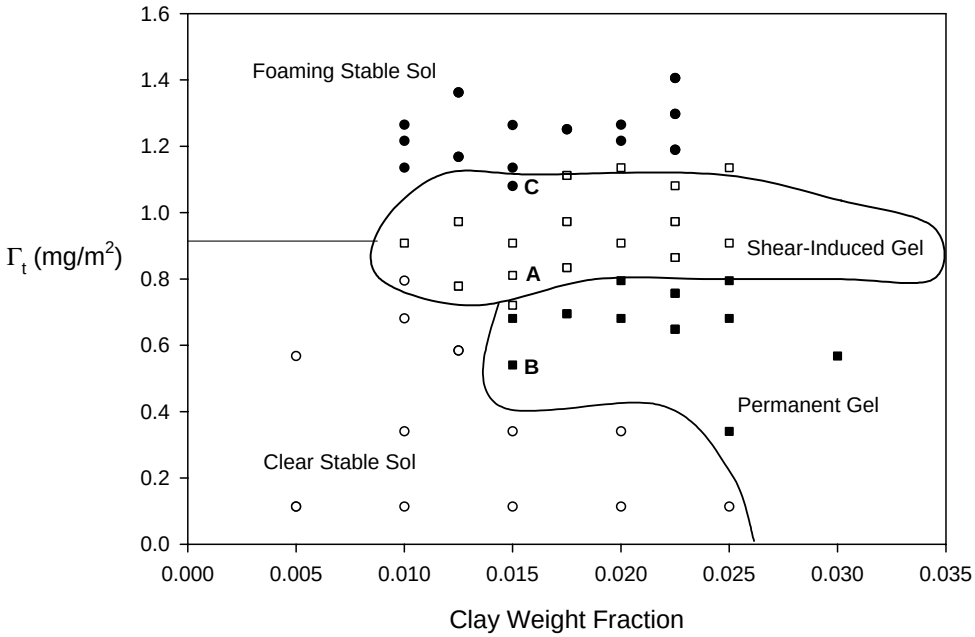

Fig. 2. Phase diagram of macroscopic behavior for the Laponite–PEO system as function of particle and polymer concentration (mg PEO per m^2 clay surface). The solid lines are included to aid in the visualization of the different phase regions.

thickness varies with the polymer molecular weight but the shell normal to the particle remains constant. These results seem to indicate that the polymer tails and loops may extend further through the edges than normal to the particle. The authors also obtained a value for the saturation adsorbed amount of 0.7 mg/m^2 for PEO chains, which reinforces the results shown in this work. The agreement of the saturation surface coverage is evidence of similarity to the mechanism proposed by Cabane et al. for the mechanical gelation in the silica–PEO system [3]. At very low Γ_t the samples behave like clay dispersions since there is too little polymer to result in any observable flocculation. When the Γ_t is increased further, the polymer forms large numbers of stable bridges with the unsaturated clay surface. This causes the macroscopic gelation of the samples that show no time-dependent relaxation because the bridges are stable in the absence of shear. At higher Γ_t, near the surface saturation value, there is little free clay surface and the aggregates are smaller because the number of bridging chains is reduced. However, the aggregates are large enough to be influenced by experimental shear rates and they can be stretched or deformed. This results in the exposure of additional free surface and creates the necessary conditions for further aggregation. This is where the shear gelation or shake-gel effect is observed. Fig. 2 shows that the samples exhibit shear-induced gelation (open squares) over a narrow range of Γ_t. When the values of Γ_t are substantially above the surface saturation values, there is free polymer in solution. This excess polymer reduces the size of the aggregates by further saturating the clay surface and preventing bridging. Additionally, it competes with other aggregates for surface that is exposed through shear.

It is also observed that the nature of the applied shear field has a profound effect on the sample behavior. When the samples are subject to simple shear in Couette flow it is found that the gels are not induced at shear rates up to thousands of inverse seconds. However, the gelation phase transition is observed with moderate manual agitation which corresponds to a significantly smaller shear rate ($<10^2$ l/s) [19]. This observation indicates that the large, stable, clay aggregates become oriented in the shear field as they form and this prevents their further aggregation in simple flow fields by reducing the number of effective collisions. This argument is in contrast to observations in the system consisting of silica particles and PEO which showed gelation under simple shear at moderate shear rates [3]. The nature of this effect is likely due to the primary particle anisotropy of the clay. On the other hand, it is found that after inducing the gel phase in the polymer clay system this state is sustained in a simple shear field with no sample relaxation. This effect is observed as long as the sample is not allowed to relax beyond a threshold value after which the phase transition cannot be induced again under simple shear.

3.2. Gel rheology

Because of the history dependence and the fast dynamics of the metastable gel, typical rheological characterization techniques become complicated. Additionally, it is found that the gelation transition could only be induced in situ by dynamic experiments at large amplitudes and frequencies. Under these conditions the time needed for shear gelation is unpredictable and accurate mechanical measurements are prevented. Therefore, to probe the relaxation of the gel

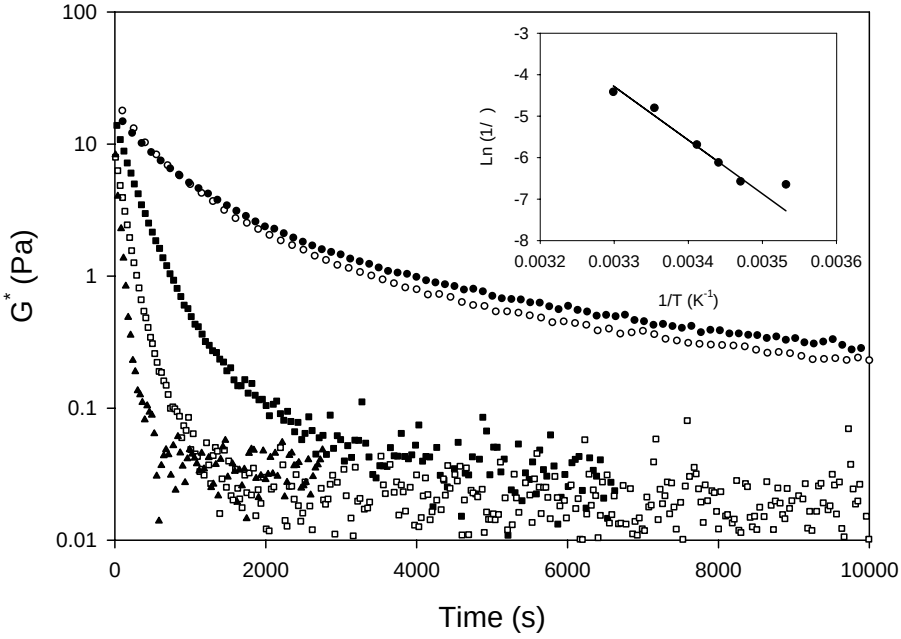

Fig. 3. Semi-log plot of relaxation after sheared induced gelation for 300 K PEO 0.45% (w/w) and Laponite 1.5% (w/w) (sample A in Fig. 2) at various temperatures. 10 °C (filled circles), 15 °C (open circles), 20 °C (filled squares), 25 °C (open squares), 30 °C (filled triangles). Insert: Arrhenius plot of the initial relaxation time.

state, we developed a specific protocol that generates a reproducible history. The samples are first induced into the gel state by manual agitation of the jars and loaded into the rheometer. The samples are then sheared for 5 min at a rate of 300 s^{-1} before characterization of the relaxation. This controlled initial shearing is carried out in order to give all tested samples the same starting condition after the manual gel induction. Experiments are also repeated to investigate the variation caused by differences in loading the samples. Repetition of experiments is reproducible with experiment to experiment deviations on the same sample being below 10% of the signal. Probe experiments are carried out at a small strain of 1% and frequency of 1 rad/s to prevent any non-linear rheological response and to avoid excessive sample manipulation while still maintaining a reasonable signal to noise ratio during the relaxation. Our approach generates a consistent and reproducible deformation history.

Fig. 3 shows the relaxation of the magnitude of the complex modulus, $|G^*|$, for a sample at various temperatures. The drop in the modulus is observed to be more than two orders of magnitude. The shear induced phases typically have similar initial complex moduli values of 10–30 Pa which drop to values below 0.1 Pa, a value typical of dilute aqueous colloidal dispersions. Initially, the elastic component of the modulus (G') is only slightly larger than the viscous component (G'') while, after the relaxation is complete, the viscous component dominates. It is observed that the relaxation is initially exponential but becomes slower as it proceeds. A characteristic relaxation time for the initial relaxation is defined by fitting the early relaxation of the complex modulus to a single exponential decay (Eq. (3))

$$|G^*| = (G'^2 + G''^2)^{1/2} = |G^*|_0 \, e^{-t/\tau} \quad (3)$$

The relaxation experiments indicate that the process is very sensitive to the sample temperature. The characteristic relaxation time is 120 s for the samples at 25 °C and 760 s at 10 °C. When the temperature is decreased, the single exponential approximation becomes less accurate as can be observed from the increased curvature of the data in the semi-log plot. Fig. 3 indicates that at lower temperatures the relaxation is significantly slowed and actually incomplete after more than 12 h. This observation is consistent with the relaxation being due to the thermal motion of the particles and the polymer. However, it is also possible that temperature-dependent solvation in PEO–water could cause loops and tails to extend further at lower temperatures than at higher ones and therefore change the aggregation morphology. On the other hand, SANS profiles indicate that for this temperature range there are no structural differences between gels formed at low temperatures as compared to those at higher temperatures. Additionally, we find that at even lower temperatures (5 °C) the relaxation is incomplete for periods as long as 3 days. This suggests that aggregate breakup depends on an activated process. This is confirmed by an Arrhenius plot for the characteristic relaxation times shown in the insert to Fig. 3. An activation energy of 107 kJ/mol is obtained from the slope of the line. This temperature behavior arises due to the existence of an energetic barrier for the desorption of the unstable anchoring polymer segments.

An aging effect is also observed when relaxation is probed on samples that are allowed to rest for several days. This im-

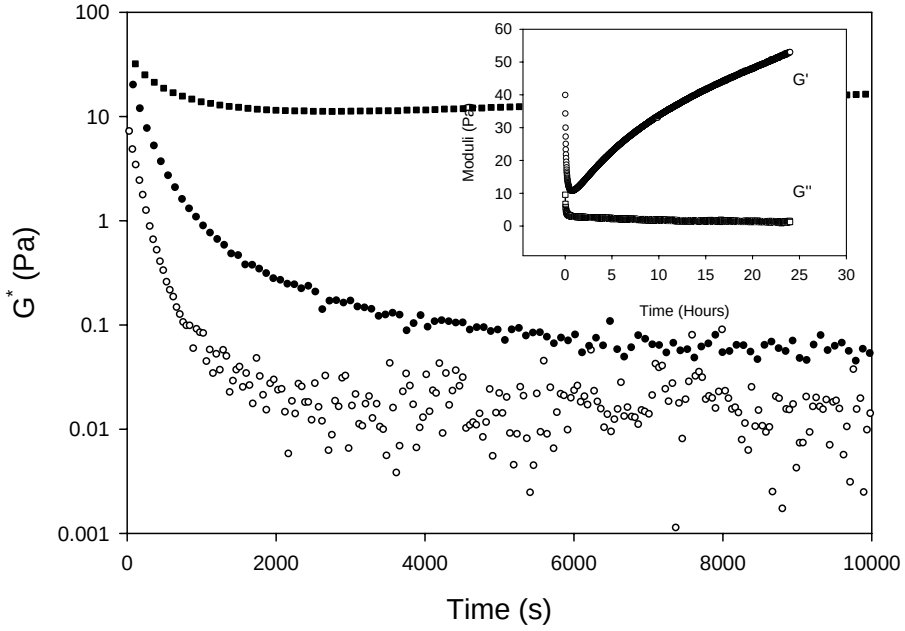

Fig. 4. Semi-log plot of relaxation after sheared induced gelation for 300 K PEO 0.45% (w/w) and Laponite 1.5% (w/w) (sample A in Fig. 2) after variable rest periods. Fresh (open circles), 7-day-old (filled circles), 21-day-old (filled squares) sample. Insert: expanded time axis for 3-week-old sample showing "Laponite type" gel restructuring after shear gelation and relaxation.

plies that the aggregates are still able to form the clay-type gel by repositioning themselves in solution. PEO-containing samples that are allowed to rest for weeks form transparent thick gels similar to those of pure Laponite dispersions. When these samples are agitated the shear thickening behavior is still observed but the relaxation is significantly slower and incomplete. As with pure clay dispersions, the aging behavior is faster for samples that contain larger clay concentrations. For samples containing clay concentrations above 2 wt.%, the aging behavior is observable within a day. Therefore, our experiments are carried out at a clay concentration of 1.5 wt.% because this concentration allows the decoupling of the shear induced gelation from the stable aging effect while still having measurable rheological property changes. Fig. 4 shows the gel relaxation for identical samples measured immediately after preparation and after 1 and 3 weeks of rest at 25 °C. One week after preparation, the slower and incomplete relaxation is evident already. The 3-week-old sample shows clay-type gelation on the timescale of the experiment. The insert in Fig. 4 shows an expanded time axis that depicts the two very different time scales of the different gelation mechanisms. In contrast to simultaneous growth of G' and G'' in the shear induced gel, this clay-type gelation is characterized by the increase of the elastic modulus (G') with a constant loss modulus (G''). These stable gels also have a greater mechanical strength than the shear induced gel phase.

Lissajous phase plots of the strain versus stress signals are collected during the relaxation to observe the linearity of the response. A linear response of the sample yields an elliptical pattern that becomes a line in the limit of a Hookean solid and a full circle in the limit of the Newtonian viscous fluid [20]. Deviations from elliptical shapes are indications of non-linear responses and higher harmonics that can arise due to the material properties or to instrument effects like wall slip. Relaxation experiments carried out with relatively small strain values ($\gamma \leq 10\%$) show linear behavior throughout the relaxation. However, when the phase plots are collected at large strain amplitudes ($\gamma > 100\%$) the response goes through a non-linear region during the relaxation. Fig. 5 illustrates the Lissajous phase plots for a strain of 500%. The torque values are divided by the maximum torque in the cycle to directly compare the shapes of the figures. It is observed that the response of the fluid is linear at short and long relaxation times but experiences a non-linear intermediate region during the relaxation. The same observation of a transient non-linear regime is made for strain amplitudes of 100%. While the gel and relaxed sol structures appear to be rheologically robust, the sample structure appears to pass through a very sensitive region during the relaxation. This non-linear response may result from a region where the sample properties are such that wall slip becomes significant, or simply be due to the result of a structure that is more sensitive to mechanical deformation. It is difficult to imagine that slip would be evident in transient structures but not in the gelled state. It is more likely that the non-linearity of the Lissajous phase plots indicates a more sensitive structure exists during the relaxation.

Schmidt et al. carried out optical and rheological measurements on more concentrated clay gels in the presence of larger PEO chains of $M_w = 10^6$ g/mol [13]. The authors report a shear-thinning response for all accessible shear rates

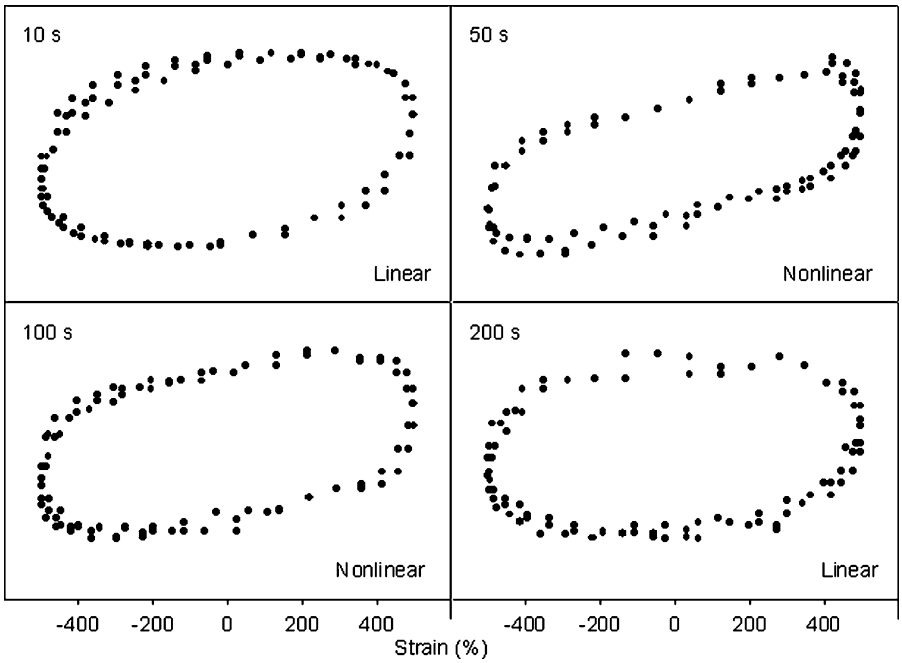

Fig. 5. Lissajous plot for the relaxation of 300 K PEO 0.45% (w/w) and Laponite 1.5% (w/w) (sample A in Fig. 2) at 25 °C with a strain amplitude of 500%. The torque measurements were normalized vertically with the maximum torque in the cycle. At large measurement amplitudes the response is initially linear, goes through a non-linear regime and again becomes linear after the structure relaxation has finished.

and stresses. Interestingly, the authors find experimental difficulties on testing the sample containing the lowest polymer concentrations (LRD1 in reference [13]). The observations of shear induced phase separation, turbidity and wall-slip are somewhat consistent with the formation of a "shake gel". The sample is likely at the edge of the shear-induced gelation boundary and close to surface saturation. However, the samples used in the study contain clay concentrations that are above the stable gelation concentration and it is therefore hard to discriminate between the shear-induced gelation and

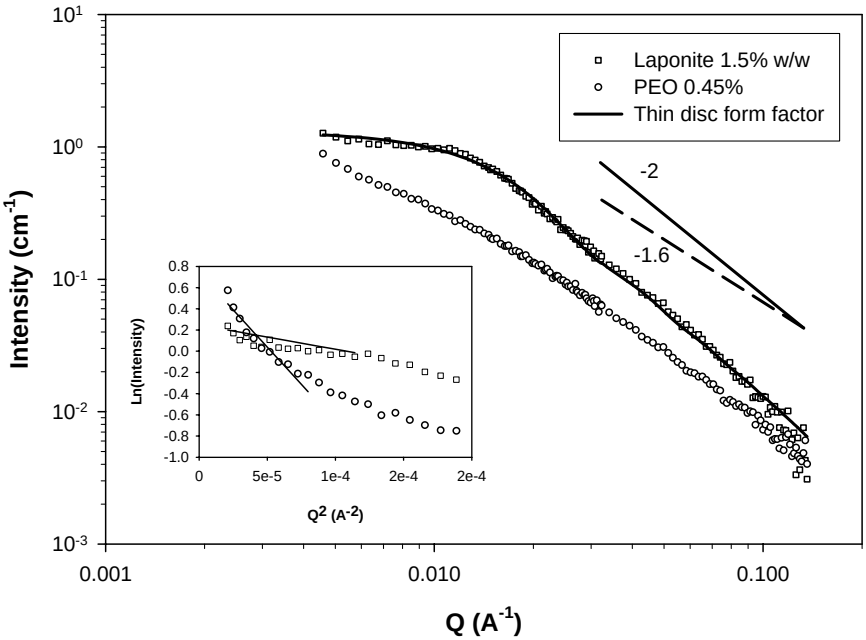

Fig. 6. Scattering profiles for 1.5% Laponite clay (squares) and 0.45% PEO (circles) in pure D_2O. The PEO curve was vertically shifted for clarity. The clay profile is characteristic of fully dispersed thin discs of 30 nm diameter (solid line). Slopes of −2 and −1.6 are observed high Q which are typical of thin particles and excluded volume random chains, respectively. Insert: corresponding Guinier fits.

the formation of the stable clay network. The effects due to adsorption in the nanoparticle size range also become evident in the reported paper. The scattering [14], rheology and birefringence [13] results are suggestive of a dynamic network with equilibrium polymer adsorption and desorption. This is only possible because the constrained surface only allows few segments to act as anchors and the adsorption is reversible on short timescales.

3.3. Small angle neutron scattering

Fig. 6 shows the scattering profile for a 1.5% (w/w) dispersion of clay platelets in D_2O which follows a slope of -2 at $Q > 0.02\,A^{-1}$. The slope is indicative of scattering from thin two-dimensional structures. Moreover, the excellent agreement between the low Q data and the form factor for non-interacting thin discs (solid line) [21], indicates that freshly prepared samples of Laponite at these concentrations (1.5%, w/w) are still randomly oriented. The fit to the thin disc form factor resulted in a clay radius of 13.3 nm with a thickness of 0.8 nm thickness indicating complete exfoliation of the clay. The lack of structure is because of the very slow gel development that takes place over periods of several days at the lower clay concentrations. It is observed by several groups that clay dispersions of concentrations just above 2% exhibit fractal type scattering at low Q-values [10]. This is not observed in fresh samples of 1.5% (w/w) clay or lower. Laponite dispersions do not show shear anisotropy in their scattering in this Q range [14]. The insert shows a Guinier plot from which the disc radius is calculated to be 16.4 nm. In the Guinier analysis the radius of gyration can be calculated from the slope of a plot of $\ln(I)$ versus Q^2 for values of Q approaching zero and $QR_g < 1$ (Eq. (4)) [21]

$$I(Q) = I(Q = 0)\exp(-\tfrac{1}{3}Q^2R_g^2) \quad (4)$$

For thin discs, the radius of the disc is equal to $\sqrt{2}$ times the radius of gyration. Fig. 6 also shows the scattering profile for 0.45% PEO dispersed in D_2O. The scattering shows a linear dependence with a slope near -1.6 that is characteristic of random coils with excluded volume interactions [22]. The radius of gyration for the PEO chains is independently measured through scattering and viscometry to be about 20 nm which is in the same size range as the clay particles.

Fig. 7 shows the scattering profiles for 1.5% clay and 0.45% PEO in pure D_2O (sample A in Fig. 2) where all the components contribute to the scattering. The top figure is collected at 25 °C and the lower figure at 10 °C. Two data sets are shown in each figure, one is collected in the gel state as it is sheared at $300\,s^{-1}$ to prevent the sample relaxation (open squares) and the other at rest after 2 h of relaxation (open circles). The relaxation is considered complete when no further development of the profile is observed in short sequential scattering experiments. At a temperature of 25 °C the profile shows no time dependence after 2 h of relaxation. This correlates well with the measured relaxation of the complex modulus, since after 7200 s the sample is in its final fluid state. As expected for a system of particles and adsorbing polymer, we find that the low Q scattering from the mixture is larger than that from the sum of the pure components at the same contrast and concentration. We also find that the scattering profile of the sample in the relaxed state is similar in shape to that of pure clay. However, the shoulder is shifted towards higher Q-values indicating enlargement of the aggregates. We expect this is due to the adsorption of the polymeric chains and some aggregation of particles.

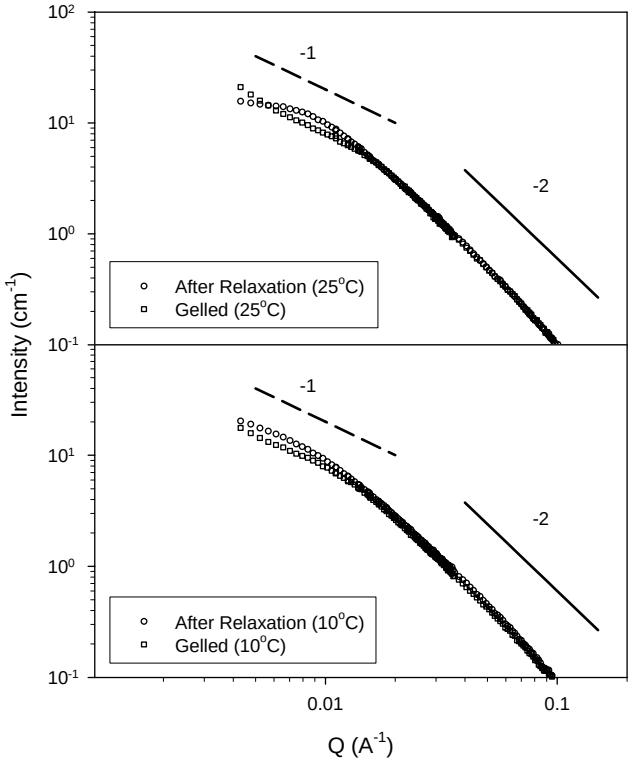

Fig. 7. Scattering from 1.5% clay and 0.45% polymer (sample A in Fig. 2) dispersed in D_2O while gelled under $300\,s^{-1}$ shear (squares) and after relaxation for 2 h at 25 °C (top) and 10 °C (bottom). No anisotropy was observed in the two-dimensional profiles at these Q ranges.

Little or no shear anisotropy in the scattering is observed for the samples in the measured Q range for shear rates as high as $1000\,s^{-1}$. Yet the samples in the induced gel state at these compositions are highly birefringent and show elongational elasticity (evidenced by pulling strong fibers when they are scooped from the sample jar). This implies that there is long-range alignment of the aggregates that should scatter at smaller Q-values. It appears then that in the size range studied, the primary particles and polymer chains are not highly oriented. The birefringence is likely due to the refractive index differences between the large elongated flocs that are shear oriented and the surrounding water. This is in contrast to shearing of concentrated networks of Laponite/PEO gels which caused the orientation of the individual polymer chains and the primary clay particles [14]. The scattering in the gel state also shows a change in slope from a value of -2 at high Q to -1 at lower Q-values. A slope of -1 is

expected for elongated or one-dimensional objects. This observation is consistent with the highly birefringent gel state which is likely due to the formation of elongated or fiber-like aggregates interacting in solvent of excess water. A similar observation was made by Cabane on the silica system where these aggregates showed anisotropy in the neutron scattering regime [3]. The aggregates were described as similar to a pearl necklace where the polymer was much larger than the beads. However, the polymer in our system is of similar size to the clay discs and it is more likely that it acts as "glue" between particles rather than as a backbone structure. Also, the elongated aggregates in this system are probably longer that those formed in the silica system since the shear-induced elasticity is observed at much lower particle concentrations.

When the experiment is repeated at a temperature of 10 °C (Fig. 7 (bottom)), we find that there is no difference between the scattering profiles of samples in the gelled state and in the state than exists after more than 10 h of relaxation. Temperature does not affect the initial structure of the gel since the scattering from the samples at 10 and 25 °C is essentially the same. Therefore relaxation must be a result of the breakup of aggregates due to their thermal fluctuations as previously anticipated [2]. At 10 °C the relaxation is incomplete and there is no evolution of the scattering because the thermal fluctuations are not strong enough to break all of the unstable aggregates. The sample is kinetically trapped in a metastable state until the temperature is increased.

When the solvent is matched in contrast to the particles (69% D_2O) we recover the scattering profiles arising from polymer–polymer correlations. In other words, the clay is invisible to the scattering even though it contributes to the structure of the polymer in solution. The scattering at these conditions includes scattering from the segments of adsorbed chains as well as scattering from the free polymer in solution. Fig. 8 shows the scattering profiles from "shake gel" samples before and after relaxation at 25 °C (Fig. 8 (top)) and 10 °C (Fig. 8 (bottom)). The slope is consistent with two-dimensional or flat adsorption, consisting mainly of trains and short loops, which yields a high Q-value of −2. The shape in the relaxed state resembles the scattering of the dispersed clay discs. Additionally, the shoulder in the scattering moves to a lower value of Q as compared to that of the pure clay. This suggests that the relaxed sample is made up of stable aggregates containing several clay discs.

Fig. 9 (top) shows the scattering profiles for a sample with lower polymer content (sample B in Fig. 2). This sample has a crumbled gelatin appearance and shows no changes in properties after agitation of the containers. There is also

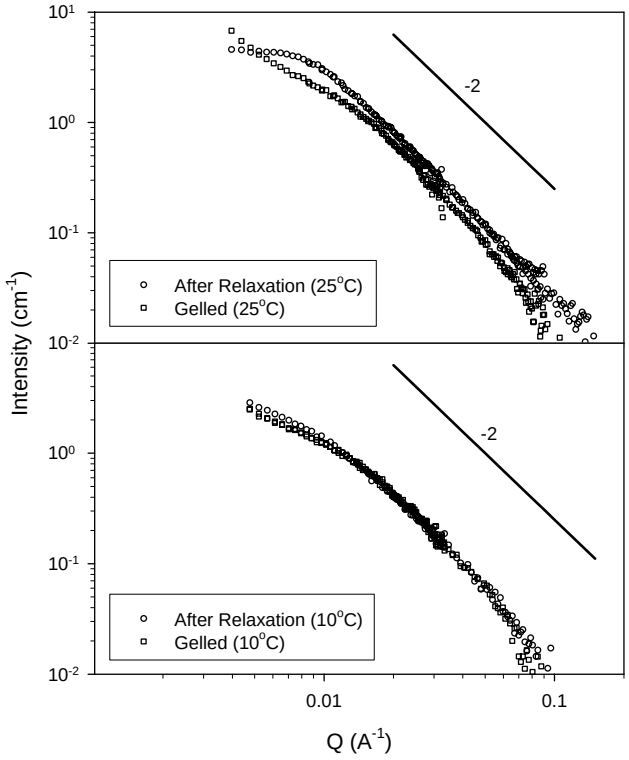

Fig. 8. Scattering from 1.5% clay and 0.45% polymer (sample A in Fig. 2) dispersed in 69% D_2O (scattering density matched to particles) while gelled at 300 s^{-1} shear (squares) and at rest after relaxation (circles) for 25 °C (top) and 10 °C (bottom). Scattering at high Q implies polymer adsorption in flat conformation.

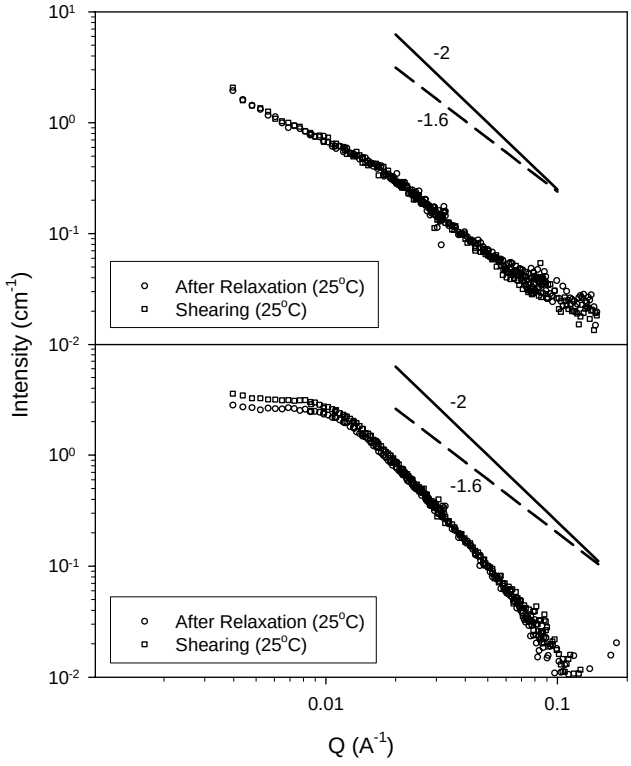

Fig. 9. Scattering from a permanently gelled sample (top, sample B in Fig. 2) and a stable foaming sol (bottom, sample C in Fig. 2), dispersed in 69% D_2O (scattering density matched to particles) under 300 s^{-1} shear (squares) and after relaxation at 25 °C (circles). There are no differences in the scattering while shearing and after relaxation. Gelled samples have high Q slopes near −1.6 showing polymer extension.

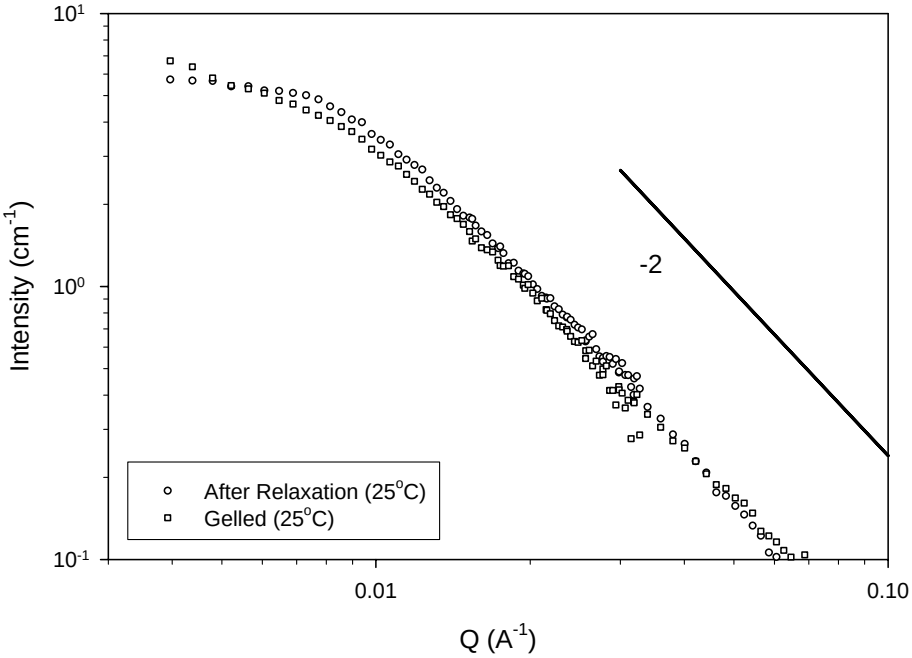

Fig. 10. Scattering from 1.5% clay and 0.45% polymer (sample A in Fig. 2) dispersed in 17% D_2O (scattering density matched to polymer) under shear at $300\,s^{-1}$ (squares) and at rest at 25 °C (circles).

no difference between the scattering functions during shear and after it is allowed to relax for a long period of time. When the solvent is matched to the particles it is found that the slope at high Q is lowered. This change in slope is caused by the highly stretched polymer bridges that form the macroscopic aggregates. As the polymers are stretched, the polymer–polymer correlation shifts from a flat adsorbed two-dimensional structure to a conformation that is closer to more extended chains and this is observed in the high Q slope change.

Scattering profiles from samples with excess polymer (sample C in Fig. 2) are presented in Fig. 9 (bottom). The profiles are almost identical in shape to the scattering of the pure dispersed clay. The similarity in scattering of the sample with excess polymer under matching conditions and the pure clay shows that the polymer closely coats the clay and adopts its shape. This confirms that the surface is saturated with polymer and aggregation is suppressed by steric stabilization. Shearing these samples has no effect on the scattering and no anisotropy is observed. When the samples are agitated a foam layer is formed that suggests the presence of free polymer chains since PEO is surface active.

Fig. 10 shows the scattering profile from a “shake gel” sample that was prepared in 17% D_2O where the scattering contrast is only between the clay particles and the solvent. The sample shows a small change in scattering profile while shearing and after relaxation at 25 °C. The decrease of the radius of gyration after relaxation shows that shear aggregation brings the clay particles closer together. However, the scattering difference is smaller than that found in the corresponding experiments with pure D_2O and with the particles contrast matched. Therefore, it is the polymer that dominates the small Q scattering and experiences the largest conformational change on aggregation.

This interesting gelation phenomenon has considerable potential in areas of industrial interest including petroleum extraction, solids filtration and materials transport. Fluids that undergo reversible gelation may prove useful as solid carriers; solid particles would remain suspended in the gelled carrier fluids as they are transported but then sediment as the fluid relaxes at rest. Oil companies, as an example, are often faced with the need to pump filler materials like sand through large distances into subterranean oil reservoirs in order to continue the oil extraction. Filtration and separation of colloidal particles may also benefit by the reversible gelation as particle filtration could be enhanced in the reversible gelation region.

4. Conclusions

Striking shear gelation behavior is observed in clay dispersions at low solids concentrations in the presence of water soluble polymer. This behavior occurs at compositions near the surface saturation limit where shear can be used to manipulate the transitions between aggregation and steric stabilization. In this narrow composition regime stable particle aggregates are deformed by shear and expose new surface area. Collisions between deformed aggregates cause the formation of unstable polymer bridges that consist of few anchoring polymer segments. The elongated aggregates in-

teract in a matrix of excess water and increase the macroscopic elasticity of the samples until shear is stopped and the polymer bridges slowly break up. Modulus relaxation and small angle neutron scattering experiments show that the relaxation process is driven by thermal motion of the polymer segments and the primary particles. Although this behavior is similar to the observed reversible shear gelation in silica and PEO, the particle anisotropy impairs the gel formation in simple shear.

The samples that show this reversible sol–gel transition also show aging characteristics that are typical of dilute clay dispersions. The properties, reversibility and time dependence of these two gels are very different and therefore this particular system shows a duality in gelation mechanisms. Although this reversible gelation has been observed with silica particles that have a different size, geometry and composition, a more systematic study with other colloid polymer systems is warranted. This will help to fully understand the shear behavior of nanoparticles in the presence of polymer at concentrations close to surface saturation.

Acknowledgements

The authors would like to acknowledge Southern Clay products for donation of the clay particles. DCP acknowledges the PPG Fellowship fund at CMU for providing funding during the completion of this work. We are above all grateful to L. Porcar, V. Prasad and D. Weitz for insightful conversations. We also acknowledge the support of the National Institute of Standards and Technology, US. Department of Commerce, in providing the neutron research facilities used in this work. This work utilized facilities supported in part by the National Science Foundation under Agreement No. DMR-9986442.

References

[1] G. Fleer, M.A. Cohen Stuart, J.M.H.M. Scheutjens, T. Cosgrove, B. Vincent, Polymers at Interfaces, Chapman & Hall, London, 1993.
[2] J. Zebrowski, V. Prasad, W. Zangh, L.M. Walker, D.A. Weitz, Colloids Surf. A 213 (2003) 189.
[3] B. Cabane, K. Wong, P. Lindner, F. Lafuma, J. Rheol. 41 (1997) 531.
[4] L.A. Harris, J.D. Goff, A.Y. Carmichael, J.S. Riffle, J.J. Harburn, T.G. St. Pierre, M. Saunders, Chem. Mater. 15 (2003) 1367.
[5] T. Cosgrove, P.C. Griffiths, P.M. Lloyd, Langmuir 11 (1995) 1457.
[6] J. Lal, L. Auvray, J. Appl. Crystallogr. 33 (2000) 673.
[7] T. Aubry, F. Bossard, M. Moan, Langmuir 18 (2002) 155.
[8] M. Aubouy, E. Raphael, Macromolecules 31 (1998) 4357.
[9] E. Hecht, H. Hoffmann, Tenside Surf. Detergents 35 (1998) 185.
[10] M. Kroon, W.L. Vos, G.H. Wedgam, Phys. Rev. E 57 (1998) 1962.
[11] B. Abou, D. Bonn, J. Meunier, Phys. Rev. E 64 (2001) 021510.
[12] C. Martin, F. Pignon, J.M. Piau, A. Magnin, P. Lindner, B. Cabane, Phys. Rev. E 66 (2002) 021401.
[13] G. Schmidt, A.I. Nakatani, C.C. Han, Rheol. Acta 41 (2002) 45.
[14] G. Schmidt, A.I. Nakatami, P.D. Butler, C.C. Han, Macromolecules 35 (2002) 4725.
[15] A. Mourchid, E. Lecolier, H. Van Damme, P. Levitz, Langmuir 14 (1998) 4718.
[16] A. Nelson, T. Cosgrove, Langmuir 20 (2004) 2298.
[17] J. Brandrup, E.H. Immergut, Polymer Handbook, Wiley/Interscience, New York, 1989.
[18] G.C. Straty, H.J.M. Stanley, C.J. Glinka, J. Statist. Phys. 62 (1991) 1015.
[19] C.W. Macosko, Rheology, VCH, New York, 1993.
[20] C. Daniel, I.W. Hamley, M. Wilhelm, W. Mingvanish, Rheol. Acta 40 (2000) 39.
[21] A. Guinier, G. Fournet, Small-Angle Scattering of X-Rays, Wiley, New York, 1955.
[22] J.S. Higgins, H.C. Benoit, Polymers and Neutron Scattering, Oxford University Press, Oxford, 1994.